Research Article

pH-Responsive Starch-Citrate Nanoparticles for Controlled Release of Paracetamol[†]

Suk Fun Chin[1], Ain Nadirah Binti Romainor[1], Suh Cem Pang[1], Boon Kiat Lee[2] and Siaw San Hwang[2]

[1] Faculty of Resource Science and Technology, Universiti Malaysia Sarawak, 94300 Kota Samarahan, Sarawak, Malaysia

[2] Faculty of Engineering, Computing and Science, Swinburne University of Technology Sarawak Campus, Malaysia

*Corresponding author's e-mail: sukfunchin@gmail.com

[†]This article has been accepted for publication and undergone full peer review but has not been through the copyediting, typesetting, pagination and proofreading process, which may lead to differences between this version and the Version of Record. Please cite this article as doi: [10.1002/star.201800336]

Received: December 5, 2018 / Revised: April 11, 2019 / Accepted: May 14, 2019

ABSTRACT

Starch-citrate samples with degrees of substitution (DS) ranging from 0.11 to 0.90 were synthesized by a green esterification reaction between citric acid and native sago starch (*Metroxylon sagu*) in an aqueous medium. Starch-citrate nanoparticles with mean diameter of 105 nm were subsequently obtained by controlled precipitation through drop-wise addition of dissolved starch-citrate solution into excess absolute ethanol. These nanoparticles were observed to exhibit pH-responsive release profiles within the physiological pH range of 1.2 to 8.6. The release profile of a model drug (paracetamol) was observed to obey the zero-order kinetics, with the release mechanism based on the diffusion and swelling model. The cytotoxicity study in HaCaT cell lines (human skin cells) showed that starch-citrate nanoparticles were non-toxic and hence are suitable for biomedical applications as pH-responsive drug carriers.

Keywords: starch-citrate nanoparticles, pH-responsive, drug release profiles, cytotoxicity

1. Introduction

pH-responsive drug delivery is an attractive mode as drugs can be selectively released in a controllable manner to pH-specific organs. This is in view of the fact that in the human body, pH values vary between organs and tissues. For instance, stomach has a pH of 1-3 while the ileum pH is 6.6-7.5 [1]. pH-responsive drug carriers have been used to prevent the initial burst release of drugs in acidic physiological conditions, and to enable release of the drug at the intended site, as well as to increase the therapeutic effect [2].

Starch is a promising precursor material for the fabrication of pH-responsive drug carriers because it is renewable, readily available, non-toxic, biodegradable, and physiologically biocompatible in nature [3]. Studies done by Zhang et al. [4] showed that pH-responsive starch-grafted poly(L-glutamic acid) nanoparticles prevented the initial burst release of insulin at pH 1.2 and increased insulin absorption at pH 6.8. Shalviri et al. [5] have synthesized pH-responsive poly(methacrylic acid)-polysorbate80-grafted starch (PMMA-PS 80-g-St) nanoparticles for the delivery of doxorubicin (an anticancer drug). Recently, the use of doxorubicin-loaded hydrazine-modified starch-coated magnetite nanoparticles as pH-responsive drug carriers in the treatment of cancer has been described [6]. Although there were several reports on the synthesis of pH- responsive starch nanoparticles, most of these involved grafting of synthetic polymers onto starch molecules, making them unfavourable for biomedical applications.

In this study, the preparation of starch-citrate nanoparticles as pH-responsive drug carriers was reported. Citric acid was attached to starch molecules to confer pH-responsiveness because it is nontoxic, safe for consumption, and highly water-soluble. The resulting starch-

citrate is water soluble and hence, there is no need to use harsh solvents for the dissolution of starch citrate. The potential utility of starch-citrate nanoparticles as drug carriers was evaluated by loading paracetamol as the model drug. The release kinetic profiles were determined in a simulated human gastrointestinal tract (GIT) with the pH of the release media being 1.2 (stomach), 7.4 (venous blood), and 8.6 (intestinal fluid). Cytotoxicity effect of the starch-citrate nanoparticles was investigated using HaCaT cell lines (human skin cells) as *in vitro* model.

2. Materials and methods

2.1. Materials

Native sago starch powder was purchased from a grocery store in Kuching (Sarawak, Malaysia). Paracetamol (trade mark: Panadol®) was purchased from a pharmacy in the same city. Absolute ethanol, disodium hydrogen phosphate and hydrochloric acid (HCl) 37% were procured from HmbG Chemicals (Hamburg, Germany). Citric acid monohydrate, sodium dihydrogen phosphate monohydrate, sodium hydroxide (NaOH) and potassium bromide (KBr) of infrared spectroscopy grade were acquired from Merck (Darmstadt, Germany). Sodium hyphophosphite monohydrate (HSP) crystals were purchased from J.T. Baker (Republic of China). HaCaT cell lines (human skin cells) were obtained from cell culture lab, Faculty of Engineering, Computing and Science, Swinburne University of Technology Sarawak Campus, Malaysia. Dulbecco's modified eagle medium (DMEM), 10% Fetal bovine serum and 1% penicillin-streptomycin were purchased from Sigma Aldrich (USA). CellTiter 96® Aqueous One Solution Cell Proliferation Assay (MTS solution) was acquired from Promega (USA). All

chemicals were used without further purification. Ultrapure water (18.2 MΩ·cm, 25 ^{o}C) was obtained from the Water Purifying System (ELGA, Ultra Genetic).

2.2. Synthesis of starch-citrate and starch-citrate nanoparticles

Starch-citrate was synthesized by an esterification reaction between sago starch and citric acid in an aqueous medium. Various amounts of sago starch powder were dispersed in ultrapure water (UPW), heated at 90 ^{o}C for 30 minutes and subsequently cooled to room temperature to form starch solutions (0.5, 1, 2, 3% (w/v)). Then, citric acid (1, 3, 4, 6, 8, 10% (w/v)) and HSP catalyst (0.35 g) were added into each of the starch solutions. The mixtures were maintained at different temperatures (30, 60, 70, 90, 100 and 120 ^{o}C) under magnetic stirring for variable durations (15, 25, 30, 35, 45, 55 and 60 minutes) to obtain starch-citrate solution. The resulting starch-citrate solution was added drop-wise into absolute ethanol in the ratio of 1:20 (v/v) under magnetic stirring to produce starch-citrate nanoparticles *via* precipitation. The precipitated nanoparticles were then centrifuged, washed with absolute ethanol (to remove excess citric acid) and dried in an oven at 60 ^{o}C for 24 hours [7].

2.3. Characterization of starch-citrate and starch-citrate nanoparticles

Fourier transformed infrared (FTIR) spectra of samples were obtained from sample/ KBr pellets, using FTIR spectrometer (Thermo Scientific Nicole iS10) at wavenumbers ranging from 400-4000 cm^{-1}. The morphology of starch-citrate nanoparticles was observed *via* scanning electron microscope (SEM) (JEOL, JSM-6390 LA) and field emission scanning electron microscopy (FESEM) (LEO, 1525). The mean particle diameter of nanoparticles was

determined by measuring the diameters of at least 100 discrete and spherical nanoparticles using the "Smile View" software of SEM. An appropriate amount of nanoparticles was dispersed in absolute ethanol by sonication and then dropped onto the fomvar-coated copper grids. TEM micrographs of the nanoparticles were obtained *via* transmission electron microscope (TEM) (JEOL Model 1230).

The swelling property of starch-citrate nanoparticles was studied by immersing pre-weighted dried starch-citrate nanoparticles in phosphate buffer solution (PBS) of various pH values (1.2, 7.4 and 8.6) at 37 ^{o}C. At predetermined time intervals (1-72 hours), samples were taken out from the buffer solution, dried with filter papers and weighed. The swelling ratio of starch citrate-nanoparticles was calculated using Equation (1):

$$\text{Swelling ratio (g/ g)} = \frac{W_s - W_d}{W_d} \quad \text{---------- (1)}$$

where W_s is the weight of swollen starch-citrate nanoparticles and W_d weight of dried starch nanoparticles in grams (g) [8].

The degree of substitution (DS) of starch-citrate sample was determined by titration [9]. About 1 g of starch-citrate was dissolved in a given volume of 0.1 M NaOH. Upon dissolution, several drops of phenolphthalein were added as an indicator. Excess NaOH was titrated with 0.2 M HCl until the color of solution changed from pink to colorless. A native starch sample was used as the blank sample. The DS of samples was calculated using Equations (2) and (3):

Percentage of substitution by citric acid (CA%) =

$$V_{NaOH} \times M_{NaOH} - (V_{blank} - V_{sample}) \times M_{HCl} \times \frac{MW_{CA}}{W_{SC}} \times 100\% \quad \text{---------- (2)}$$

$$DS = \frac{162 \times CA\ \%}{19200 - (191 \times CA\ \%)} \quad \text{---------- (3)}$$

where V_{NaOH} is the volume (mL) of NaOH while M_{NaOH} and M_{HCl} are the molarities of NaOH and HCl, respectively. V_{blank} and V_{sample} are the titrated volumes of HCl for native starch and starch-citrate, respectively. MW_{CA} is the molecular weight of citric acid and W_{SC} weight of starch-citrate used for the titration.

2.4. Loading of paracetamol onto starch-citrate nanoparticles

Various concentrations (0.5, 2, 4, 6, 8 and 10 mg/ L) of paracetamol were dissolved in 20 mL of absolute ethanol as the precipitating medium. Subsequently, 1 mL of starch-citrate solution (in a 1:8 ratio v/v) was added drop-wise and magnetically stirred for 30 minutes. During the precipitation of starch-citrate nanoparticles, paracetamol was being encapsulated within nanoparticles *via* an *in-situ* nanoprecipitation process [10].

The paracetamol-loaded starch-citrate nanoparticles were separated from the precipitating medium by centrifugation, and the absorbance of supernatant was measured using a UV-visible spectrophotometer at a wavelength of 247 nm [11]. The concentration of paracetamol which remained in the supernatant was calculated with reference to the calibration curve of paracetamol standard solutions. The loading capacity of paracetamol was calculated using Equation (4) [10]:

$$\text{Loading capacity (mg/mg)} = \frac{\text{paracetamol}_{tot} - \text{paracetamol}_{free}}{\text{weight of nanoparticles}} \quad \text{---------- (4)}$$

where paracetamol_{tot} is the total weight of paracetamol added and $\text{paracetamol}_{free}$ weight of paracetamol present in the supernatant after centrifugation.

2.5. *In vitro* drug release studies

A predetermined amount of paracetamol-loaded starch-citrate nanoparticles were weighed and placed in containers filled with 15 mL PBS. The PBS, with pH values resembling those of human stomach (1.2), blood (7.4) and large intestine (8.6), were used as the releasing media at 37 ^{o}C [12]. At predefined time intervals, 1 mL of PBS was withdrawn from each of the release media and immediately replaced with an equal volume of PBS. The absorbance values of extracted PBS solutions were analyzed using a UV-visible spectrophotometer at wavelengths ranging between 247 – 257 nm [11]. The concentrations of released paracetamol were calculated with reference to the calibration curve of standard paracetamol solutions in PBS. The percentage of paracetamol released was measured according to Equation (5) [13]:

$$\text{Drug release (\%)} = \frac{\text{paracetamol}_{rel}}{\text{paracetamol}_{load}} \text{ x } 100\% \quad \text{---------- (5)}$$

where paracetamol_{rel} is the weight of paracetamol released (mg) and $\text{paracetamol}_{load}$ weight of paracetamol loaded onto starch-citrate nanoparticles (mg).

2.6. Drug release kinetic studies

Data obtained from *in vitro* drug release studies of paracetamol from starch-citrate nanoparticles were analyzed by fitting to various kinetic models (Equation 6-10):

Zero order

$$C = C_o + k_o t \quad \text{----------} \quad (6)$$

First order

$$\ln (100-C) = \ln (C_o) - k_o t \quad \text{----------} \quad (7)$$

Higuchi

$$C = k_o \sqrt{t} \quad \text{----------} \quad (8)$$

Hixson-Crowell

$$\sqrt[3]{C_o} - \sqrt[3]{QC} = k_o t \quad \text{----------} \quad (9)$$

Korsmeyer-Peppas

$$M_t/M_\infty = k_o t^n \quad \text{----------} \quad (10)$$

where C_o, C and k_o are the initial concentration of drug, final concentration of drug and release rate constant of drug release at time (t), respectively. M_t/M_∞ is the fraction of drug released at time (t), and n is the release exponent that can be determined from the linear regression of log (M_t/M_∞) *vs* log t [14].

2.7. Cytotoxicity study

HaCaT cells were cultured in Dulbecco's modified eagle medium (DMEM) supplemented with 10% fetal bovine serum and 1（% w/v）penicillin-streptomycin incubated at 37 ºC with

5% carbon dioxide (CO_2) in humidified air. Cells were harvested and seeded in a 96-well plate and allowed to attach for 24 hours prior to addition of hydrogel solution. After overnight incubation, various concentrations (0.5, 2, 4, 6, 8, 10 mg/ mL) of starch-citrate nanoparticles dispersions were added into their respective wells. The cells were then incubated at different time points (6, 12, 24, 48, 72 hours) at 37 ºC with 5% CO_2. After the incubation, all media were removed, and MTS solution was added, followed by incubation for 4 hours. The absorbance was measured at 490 nm using BioTek microplate reader [15].

2.8. Statistical analysis

All experiments and analysis were performed in triplicate. Statistical analysis was performed using Microsoft Excel and results are expressed as mean ± standard error (SE) and n = 3.

3. Results and discussion

3.1. FTIR analysis

Citric acid was attached to starch molecule backbones *via* the esterification reaction, as shown in Fig 1. Hydroxyl (OH) groups of starch molecules reacted with the carboxylic (COOH) group of citric acid to form the ester bonds of starch-citrate molecules [16]. After esterification, an absorption peak attributed to carbonyl (C=O) ester bonds was observed in the FTIR spectrum of starch-citrate molecules at 1724 cm^{-1} and another absorption peak of the C-O stretching of the ester group was observed at 1156 cm^{-1} as shown in Fig. 2b [17, 18]. These peaks were absent in the FTIR spectrum of native starch molecules (Fig. 2a). In addition, the absorption peak of C-O-C glycosidic bonds of anhydroglucose unit (AGU) of starch molecules at 850- 854 cm^{-1} was observed to remain intact, suggesting that the aforementioned molecules

were not degraded after esterification [19]. It was revealed that peaks in the region 1648 – 1635 cm^{-1} were made up of OH group – 1648 cm^{-1} (O-H from moisture absorbency in starch) [20] and 1640 and 1635 cm^{-1} (O-H from COOH of citric acid substituted onto starch molecules) [21]. The characteristic peaks at 2931-2929 cm^{-1} indicated the presence of C-H stretching and 3445-3242 cm^{-1} was assigned to the OH groups of starch and starch-citrate molecules [22]. As shown in Fig. 2b-c, FTIR spectra for both starch-citrate and starch-citrate nanoparticles were identical, indicating that the chemical composition of starch-citrate was intact after the nanoprecipitation process.

3.2. Degree of substitution (DS) of starch-citrate

The effects of esterification conditions (such as starch concentration, citric acid concentration, reaction time and temperature) on the DS of starch-citrate were investigated. The optimum concentration of starch (1% (w/v)) was observed to yield starch-citrate with the highest DS (0.90) (Fig. 3a). As the concentrations of starch increased above 1% (w/v) the mixture became highly viscous, resulting in lower mixing efficiency during esterification and hence, starch-citrate of lower DS was obtained [23]. Fig. 3b shows that the DS of starch-citrate increased substantially from 0.23 to 0.90 as the concentration of citric acid was increased from 1 to 8% (w/v). This could be attributed to the fact that more citric acid molecules were available for esterification with the OH moieties of starch molecules. The DS of starch-citrate was observed to level off as the citric acid concentration was increased beyond 8% (w/v) because the optimum concentration had been achieved for the reaction. The reaction temperatures were observed to have significant effects on the DS of starch citrate. As shown in Fig. 3c, the highest DS (0.90) was achieved when the esterification reaction was carried out at 100 ^{o}C. At this

temperature, the structures of starch molecules were loosened due to complete gelatinization which enabled higher rates of hydrolysis of starch molecules. Enhanced interaction between starch and citric acid molecules could have resulted in the formation of starch-citrate with higher DS. However, when the temperature of the reaction was increased to 120 ^{o}C, the DS of starch-citrate became adversely affected. Beyond the optimum temperature, the crystalline structure of starch granules could have broken apart due to the thermal degradation of starch. [24]. Fig. 3d shows that reaction duration of 30 minutes was ideal for maximizing effective collisions between citric acid and starch molecules in order to achieve the highest DS of 0.90. Beyond that duration, starch molecules began to degrade.

3.3. Drug-loading capacity of starch-citrate nanoparticles

As shown in Fig. 4a, native sago starch granules were mostly large, oval and granular, with granule diameters of around 20-40 μm. Starch-citrate nanoparticles, which were obtained after nanoprecipitation, were spherical with a mean particle diameter of 105 nm as shown in the FESEM and TEM micrographs, respectively (Fig.4b and 4c). The starch-citrate nanoparticles were used for the FESEM and TEM analysis were derived from starch-citrate with 0.9 degree of substitution. Fig. 5 shows that the loading capacity of paracetamol onto starch nanoparticles increased almost linearly from 1.00 to 5.00 mg/mg as the concentration of paracetamol was increased from 0.5 to 4 mg/L. When the concentration of paracetamol was 4 mg/L, a maximum loading capacity of 5.00 mg/mg was attained, and remained constant even though concentration of paracetamol was further increased to 10 mg/L. The drug-loading capacity plateau could be attributed to the saturation of the adsorption sites of starch-citrate nanoparticles [25].

Previous studies on the possibility of drug-loading onto nanoparticles suggested that these nanoparticles had relatively low drug-holding capacities due to the use of conventional absorption loading technique [26]. Reddy and Sailaja [27] supported that the aspirin-loading capacity of ethyl cellulose nanoparticles was 0.35 mg/mg. Meanwhile, Anirudhan et al., [28] showed that the loading capacity of monthmorillonite/N(carboxyacyl) chitosan-coated magnetite nanoparticles for paracetamol was 9.60×10^{-4} mg/mg. It is noteworthy that starch-citrate nanoparticles displayed a much higher loading capacity of 5.00 mg/mg for paracetamol.

The *in-situ* nanoprecipitation drug-loading technique demonstrated a higher drug-loading capacity compared to conventional absorption methods [10]. In the former technique, paracetamol dissolved in ethanol (non-solvent system), was being entrapped in the starch-citrate solution (solvent system) during the formation of starch-citrate nanoparticles. This process occurred through precipitation and fast diffusion between the solvent and non-solvent systems [29]. Hence, the drug could be easily incorporated into nanoparticle carriers, thereby enhancing their drug-loading capacity. Besides, intermolecular interactions between drug molecules and carriers also influenced the drug-loading capacity of the latter [30]. The electrostatic interactions between COO^- groups of starch-citrate nanoparticles and $-OH_2^+$ (leaving group of paracetamol due to protonation of OH of paracetamol occurred when in contact with starch-citrate solution) during nanoprecipitation explained the high paracetamol-loading capacity of starch-citrate nanoparticles [28].

3.4. Drug release studies

Fig. 6a shows the swelling behavior of the starch-citrate nanoparticles at pH 1.2, 7.4 and 8.6 while Fig. 6b shows the release profiles of paracetamol from starch-citrate nanoparticles at the aforementioned pH values. Paracetamol release profiles were observed to be dependent on the swelling behavior of starch-citrate nanoparticles, which was in turn influenced by the pH of the releasing medium. The pH-responsiveness could be due to the difference in the protonation states of starch-citrate nanoparticles.

At pH 1.2, paracetamol was released from starch-citrate nanoparticles in a slow and sustained manner over a duration of 32 hours without any initial burst release being observed. The slower rate of drug release could be due to the smaller swelling ratio (3.2 g/g) of starch-citrate nanoparticles in acidic medium (Fig. 6a), associated with the stronger interaction of hydrogen bonds among COOH functional groups of the starch-citrate nanoparticles [31]. Paracetamol release rates were observed to be more rapid at pH 7.4 (0.38 mg/h) and pH 8.6 (0.50 mg/h) as compared to pH 1.2 (0.18 mg/h) (Fig. 6b (i), (iii) and (v)). Complete release of paracetamol from starch-citrate nanoparticles at pH 7.4 and 8.6 occurred within 16 hours and 12 hours, respectively. However, only 58% of paracetamol was released at pH 1.2 after 16 hours. The faster drug release rate at higher pH was due to the deprotonation of COOH groups of the starch-citrate nanoparticles to form COO^-, leading to electrostatic repulsion, and in turn, substantially higher swelling ratios of 45.9 g/g and 56.8 g/g at pH 7.4 and 8.6, respectively (Fig.6a) [28].

For comparison, the release behavior of tablet forms of paracetamol was investigated at different physiological pH (1.2, 7.4 and 8.6), as shown in Fig. 6b. At pH 1.2, paracetamol in tablet form released almost 100% of the drug within 4 hours (Fig. 6b (ii)). In contrast, at pH 7.4 and 8.6, the tablets disintegrated and abruptly released 100% of the drug within 1 hour (Fig. 6b (iv) and (vi)). This implies that paracetamol tablets underwent brisk drug release (with an initial burst) instead of controlled and sustained release pattern as observed in the case of starch-citrate nanoparticles (Fig. 6b (i), (iii) and (v)).

3.5. Drug release mechanism

The drug release data was fitted to various kinetic models as shown in Table 1. The correlation coefficients (R^2) of paracetamol released from starch-citrate nanoparticles in all three simulated gastrointestinal tract (GIT) pH media were nearly 1, indicating that the release profiles strongly correlated with the zero-order kinetic model. The aforementioned release profiles were dominated by simultaneous swelling and erosion of the polymer matrix which enabled diffusion of the drug from starch-citrate nanoparticles. Higher regression (R^2) values (0.9043-0.9987) was observed for Hixson-Crowell and Higuchi models (Table 1) [32]. The Korsmeyer-Peppas model was applied to further confirm the paracetamol release mechanism from starch-citrate nanoparticles [33]. The R^2 values of the Korsmeyer-Peppas equation were 0.9889, 0.9687 and 0.9717 for pH 1.2, 7.4 and 8.6, respectively. This showed that drug release was driven by diffusion of paracetamol molecules out of the starch-citrate nanoparticles matrix. The release mechanism was determined from the slope value (n) of Korsmeyer-Peppas equation. The n values of the releasing media (pH 1.2, 7.4 and 8.6) fell within the range of 0.5-

1.0, indicating that the release of paracetamol from starch-citrate nanoparticles was governed by non-Fickian release behavior, as well as induced by diffusion through the swelling of starch-citrate nanoparticles [34].

3.6. *In vitro* cytotoxicity assay

The starch-citrate nanoparticles were screened for cytotoxic effect *via* MTS [3-(4,5-Dimethylthiazol-2-yl)-5-(3-carboxymethoxyphenyl)-2-(4-sulfophenyl)-2H-tetrazolium] based colorimetric assay using HaCaT cells at various concentrations and time points. Pursuant to ISO 10993-5 (practical guidelines for cytotoxicity), percentage of cells viability above 80% are considered as non-cytotoxicity. As seen in Fig. 7, nanoparticles at low concentrations from 0.5 – 6 mg/mL showed no cytotoxicity on HaCaT cells until 48 hours of incubation time and percentage of cells viability were above 100% [15, 35]. There was slight cytotoxic effect observed with percentage of cells viability range was within 70-100% at 6 and 8 mg/mL of nanoparticles, 72 hours, and various incubation time respectively. However, percentage of cells viable was below than 50% at the highest concentration of 10 mg/mL as shown in Fig. 7. Based on ISO 10993-5 cytotoxicity guidelines, nanoparticles at this concentration were cytotoxic towards HaCaT cells [35].

The possible factor that caused cell death at 10 mg/mL was most likely due to the nature of nanoparticles chemical state (excess of hydrogen ions at high concentration of nanoparticles solution make the solution acidic), whereas pH value of the nanoparticles was at around pH 4 – 5, which is incompatible with the cell growth. In cell culture, pH regulation is crucial as most cells grow well or cellular metabolic activities occurs at optimal pH in between 7 – 8. Cells are

usually grown in medium at pH 7.4 that employs a buffering system with probable increasing and reduction at both ends of the optimal pH range [36]. Cells were therefore not able to sustain growth at low pH of 4-5. Cellular activities were disrupted by any drastic change in the pH level. The lower concentrations of nanoparticles at pH level of around 7 to 8 was the optimal condition for cell growth and hence no cytotoxic effect was observed. Starch-citrate nanoparticles did not exhibit cytotoxic effect towards HaCaT cells at various low concentrations, thus indicating the potential of starch-citrate nanoparticles in biomedical application [37].

4. Conclusions

Paracetamol-loaded pH-responsive starch-citrate nanoparticles were successfully prepared by the nanoprecipitation method. The synthesis conditions used are aqueous-based without the use of harsh organic solvents. Starch-citrate nanoparticles exhibited comparatively higher drug loading capacity which could be associated with the drug loading technique employed in this study. The swelling ratio of starch-citrate nanoparticles showed strong dependent on the medium pH, which collectively determined their drug release kinetic profiles. Release kinetic studies of paracetamol from starch-citrate nanoparticles suggested that: (1) the release profile followed the zero-order kinetic model, and (2) the drug release mechanism entailed a combination of diffusion and swelling of the starch-citrate nanoparticles. Cytotoxicity study demonstrated that starch-citrate nanoparticles were low in toxicity and could be a promising pH-responsive nano-carriers for targeted drug delivery.

Conflict of interests

The authors declare that there is no conflict of interests regarding the publication of the paper.

Acknowledgement

Financial support from Ministry of Education, Malaysia *via* the award of a fundamental research grant [FRGS/STG02(02)/1116/2014(02)] and MyBrain15 (MyPhD) for graduate scholarship programme are gratefully acknowledged.

Novelty of the work

- Starch-citrate nanoparticles are a new type of pH responsive nanoparticles
- pH-responsive starch-citrate nanoparticles could prevent the initial burst release effect of the drug in acidic medium.
- Since pH-responsive starch-citrate nanoparticles are demonstrated to be low toxicity, its potential application as drug delivery carriers are envisaged.

References

[1] S. Bazban-Shotorbani, M.M. Hasani-Sadrabadi, A. Karkhaneh, V. Serpooshan, K.I. Jacob, A. Moshaverinia, M. Mahmoudi, Revisiting structure-property relationship of pH-responsive polymers for drug delivery applications, *J. Control Release* 2017, *253*, 46-63.

[2] B. Tian, S. Liu, S. Wu, W. Lu, D. Wang, L. Jin, B. Hu, K. Li, Z. Wang, Z. Quan, pH-responsive poly (acrylic acid)-gated mesoporous silica and its application in oral colon targeted drug delivery for doxorubicin, *Colloids Surf. B Biointerfaces* 2017, *154*, 287-296.

[3] S.H.M. Najafi, M. Baghaie, A. Ashori, Preparation and characterization of acetylated starch nanoparticles as drug carrier: ciprofloxacin as a model, *Int. J. Biol. Macromol.* 2016, *87*, 48-54.

[4] Z. Zhang, H. Shan, L. Chen, X. Zhuang, X. Chen, Synthesis of pH-responsive starch nanoparticles grafted poly(L-glutamic acid) for insulin controlled release, *Eur. Polym. J.* 2013, *49*, 2082-2091.

[5] A. Shalviri, H.K. Chan, G. Raval, M.J. Abdekhodaie, Q. Liu, H. Heerklotz, X.Y. Wu, Design of pH-responsive nanoparticles of terpolymer of poly(methacrylic acid),polysorbate 80 and starch for delivery of doxorubicin, *Colloids Surf. B Biointerfaces* 2013, *101*, 405-413.

[6] N. Zohreh, S.H. Hosseini, A. Pourjavadi, Hydrazine-modified starch coated magnetic nanoparticles as an effective pH-responsive nanocarrier for doxorubicin delivery, *J. Ind. Eng. Chem.* 2016, *39*, 203-209.

[7] S.H. Tay, S.C. Pang, S.F. Chin, A facile approach for controlled synthesis of hydrophilic starch‐based nanoparticles from native sago starch, *Starch‐Stärke*, 2012, *64* (12), 984-990.

[8] M.N. Ranjha, U.F. Qureshi, Preparation and characterization of crosslinked acrylic acid/hydroxypropyl methyl cellulose hydrogels for drug delivery, *Int. J. Pharm. Pharm. Sci.* 2014, *6*, 400-410.

[9] S.H. Tay, S.C. Pang, S.F. Chin, Facile synthesis of starch-maleate monoesters from native sago starch, *Carbohydr. Polym.* 2012, *88*, 1195-1200.

[10] S.F. Chin, S.N.A. Mohd Yazid, S.C. Pang, Preparation and characterization of starch nanoparticles for controlled release of curcumin, *Int. J. Polym. Sci.* 2014, *2014*, 1-8.

[11] L. Bounabi, N.B. Mokhnachi, N. Haddadine, F. Ouazib, R. Barille, Development of poly (2-hydroxyethyl methacrylate)/clay composites as drug delivery systems of paracetamol, *J. Drug Deliv. Sci. Technol.* 2016, *33*, 58-65.

[12] J. Bajpai, G. Kaur Mann, A.K. Bajpai, Preparation, characterization and water uptake behavior of polysaccharide based nanoparticles, *Prog. Nanotechnol. Mater.* 2012, *1*, 9-17.

[13] G. Arora, K. Malik, I. Singh, S. Arora, V. Rana, Formulation and evaluation of controlled release matrix muchoadhesive tablets of domperidone using *Salvia plebeian* gum, *J. Adv. Pharm. Technol. Res.* 2011, *2*, 163-169.

[14] H.B. Bakrudeen, C. Sudarvizhi, B.S.R. Reddy, Starch nanocrystals based hydrogel:Construction, characterizations and transdermal application, *Mater. Sci. Eng. C.* 2016, *68*, 880-889.

[15] Q. Jiang, J. Wang, R. Tang, D. Zhang, X. Wang, Hypromellose succinate-crosslinked chitosan hydrogel films for potential wound dressing, *Int. J. Biol. Macromol.* 2016, *91*, 85-91.

[16] E. Olsson, C. Menzel, C. Johansson, R. Andersson, K. Koch, L. Jarntrom, The effect of pH on hydrolysis, cross-linking and barrier properties of starch barriers containing citric acid, *Carbohydr. Polym.* 2013, *98*, 1505-513.

[17] S.H. Classen, C.M. Müller, A.L. Parize, A.T Pires, Synthesis and characterization of cassava starch with maleic acid derivatives by etherification reaction, *Carbohydr. Polym.* 2018, *180*, 348-353.

[18] Y. Zhao, W. Shen, Z. Chen, T. Wu, Freeze-thaw induced gelation of alginates, *Carbohydr. Polym.* 2016, *148*, 45-51.

[19] S. Sukhija, S. Singh, C.S. Riar, Effect of oxidation, crosslinking and dual modification on physicochemical crystallinity, morphological, pasting and thermal characteristic of elephant food yam (*Amorphophallus paeoniifolius*) starch, *Food Hydrocoll.* 2016, *55*, 56-64.

[20] C. Menzel, G. Seisenbaeva, P. Agback, M. Gällstedt, A. Boldizar, K. Koch, Wheat starch carbamate: Production, molecular characterization, and film forming properties, *Carbohydr. Polym.* 2017, *172*, 365–373.

[21] E. Cheraghipour, S. Javadpour, A.R. Mehdizadeh, Citrate capped superparamagnetic iron oxide nanoparticles used for hyperthermia therapy, *J. Biomed. Sci. Eng.* 2012, *5*, 715-719.

[22] A. Awadhiya, D. Kumar, V. Verma, Crosslinking of agarose bioplastic using citric acid, *Carbohydr. Polym.* 2016, *151*, 60-67.

[23] S.S. Shi, G.Q. He, Process optimization for cassava starch modified by octenyl succinic anhydride, *Procedia Eng.* 2012, *37*, 255-259.

[24] F. Han, C. Gao, M. Liu, F. Huang, B. Zhang, Synthesis, optimization and characterization of acetylated corn starch with the high degree of substitution, *Int. J. Biol. Macromol.* 2013, *59*, 372-376.

[25] M. Parent, H. Baradari, E. Champion, C. Damia, M. Viana-Trecant, Design of calcium phosphate ceramics for drug delivery applications in bone diseases: A review of the parameters affecting the loading and release of the therapeutic substance, *J. Control. Release*, 2017, *252*, 1-17.

[26] S. Hao, Y. Wang, B. Wang, J. Deng, X. Liu, J. Liu, Rapid preparation of pH-sensitive polymeric nanoparticle with high loading capacity using electrospray for oral drug delivery, *Mater. Sci. Eng. C.* 2013, *33*, 4562-4567.

[27] A.S. Reddy, A.K. Sailaja, Preparation and characterisation of aspirin loaded ethylcellulose nanoparticles by solvent evaporation technique, *World. J. Pharm. Pharm. Sci.* 2014, *3*, 1781-1793.

[28] T.S. Anirudhan, S.S. Gopal, S. Sandeep, Synthesis and characterization of montmorillonite/N-(carboxyacyl) chitosan coated magnetic particle nanocomposites for controlled delivery of paracetamol, *Appl. Clay Sci.* 2014, *88*, 151-158.

[29] S. F. Chin, F. B. Jimmy, S.C. Pang, Size controlled fabrication of cellulose nanoparticles for drug delivery applications, *J. Drug Deliv Sci. Tech.* 2018, 43, 262-266.

[30] Y. Li, L. Yang, Driving forces for drug loading in drug carriers, *J. Microencapsul.* 2015, 32, 255-272.

[31] E. Badakshanian, K. Hemmati, M. Ghaemy, Enhancement of mechanical properties of nanohydrogels based on natural gum with functionalized multiwall carbon nanotube: Study of swelling and drug release, *Polymer* 2016, *90*, 282-289.

[32] L. Wang, R. Feng, J. Gao, Y. Xi, G. Huang, Generic sustained release tablets of trimetazidine hydrochloride: Preparation and *in vitro–in vivo* correlation studies, *Asian J. Pharm. Sci.* 2016, *11*, 417-426.

[33] J. Fan, F. Liu, Z. Wang, Shear rheology and *in-vitro* release kinetic study of apigenin from lyotropic liquid crystal, *Int. J. Pharm.* 2016, *49*, 248-254.

[34] S.A. Chime, G.C. Onunkwo, I.I. Onyishi, Kinetics and mechanisms of drug release from swellable and non swellable matrices: A review, *Res. J. Pharm. Biol. Chem. Sci.* 2013, *4*, 97-103.

[35] J. López-García, M. Lehocký, P. Humpolíček, P. Sáha, HaCaT keratinocytes response on antimicrobial atelocollagen substrates: extent of cytotoxicity, cell viability and proliferation, *J. Funct. Biomater.* 2014, *5*, 43-57.

[36] Y.H. Chen, S.H. Chang, I.J. Wang, T.H. Young, The mechanism for keratinocyte detaching from pH-responsive chitosan, *Biomaterials* 2014, *35*, 9247-9254.

[37] S. Baghaie, M.T. Khorasani, A. Zarrabi, J. Moshtaghian, Wound healing properties of PVA/starch/chitosan hydrogel membranes with nano zinc oxide as antibacterial wound dressing material, *J. Biomater. Sci. Polym. Ed.* 2017, *28*, 2220-2241.

Figure Captions

Fig. 1. Schematic representation of the esterification reaction of citric acid and starch to form starch- citrate molecules

Fig. 2. FTIR spectra of (a) native starch, (b) starch-citrate molecule and (c) starch-citrate nanoparticles

Fig. 3. Effect of synthesis conditions on the degree of substitution (DS) of starch-citrate molecules: (a) starch concentration, (b) citric acid concentration, (c) reaction temperatures and (d) reaction times

Fig. 4. (a) SEM image of native starch granules; (b) FESEM and (c) TEM images of starch-citrate nanoparticles（DS of 0.9）

Fig. 5. Paracetamol-loading capacity of starch-citrate nanoparticles

Fig. 6(a). Swelling ratios of starch-citrate nanoparticles in different pH of physiological media (1.2, 7.4 and 8.6) as a function of time

Fig. 6(b). Percentage of paracetamol released from starch-citrate nanoparticles and tablets in media of various pH

Fig. 7. Cell viability of HaCaT cells cultured with various starch-citrate nanoparticles concentration for 6-72 hours

Table 1: Kinetics modeling of drug release studies of paracetamol-loaded starch-citrate nanoparticles.

LIST OF FIGURE

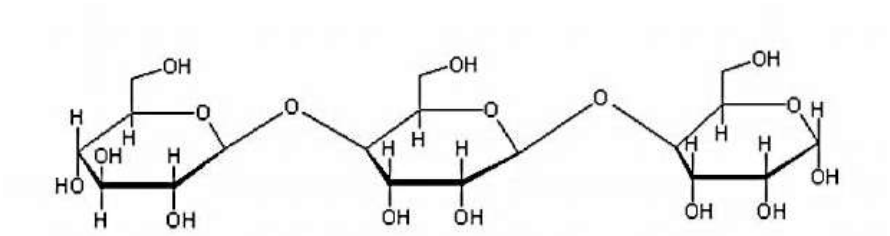

Starch

+

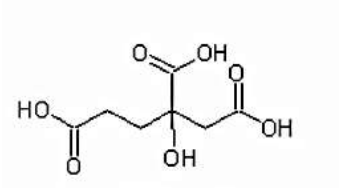

Citric acid

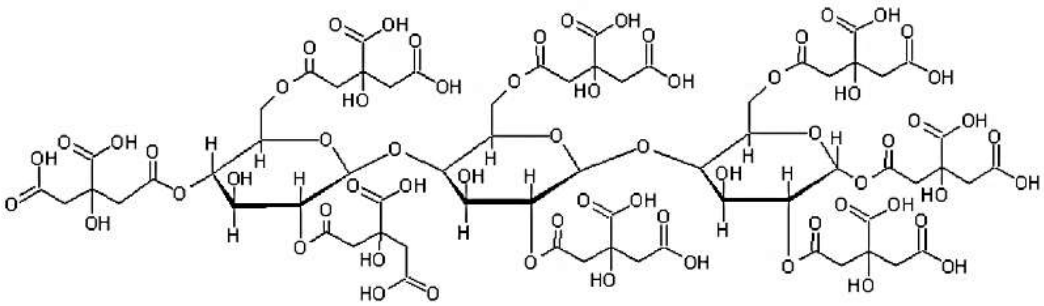

Starch-citrate

Fig. 1. Schematic representation of the esterification reaction of citric acid and starch to form starch- citrate molecules

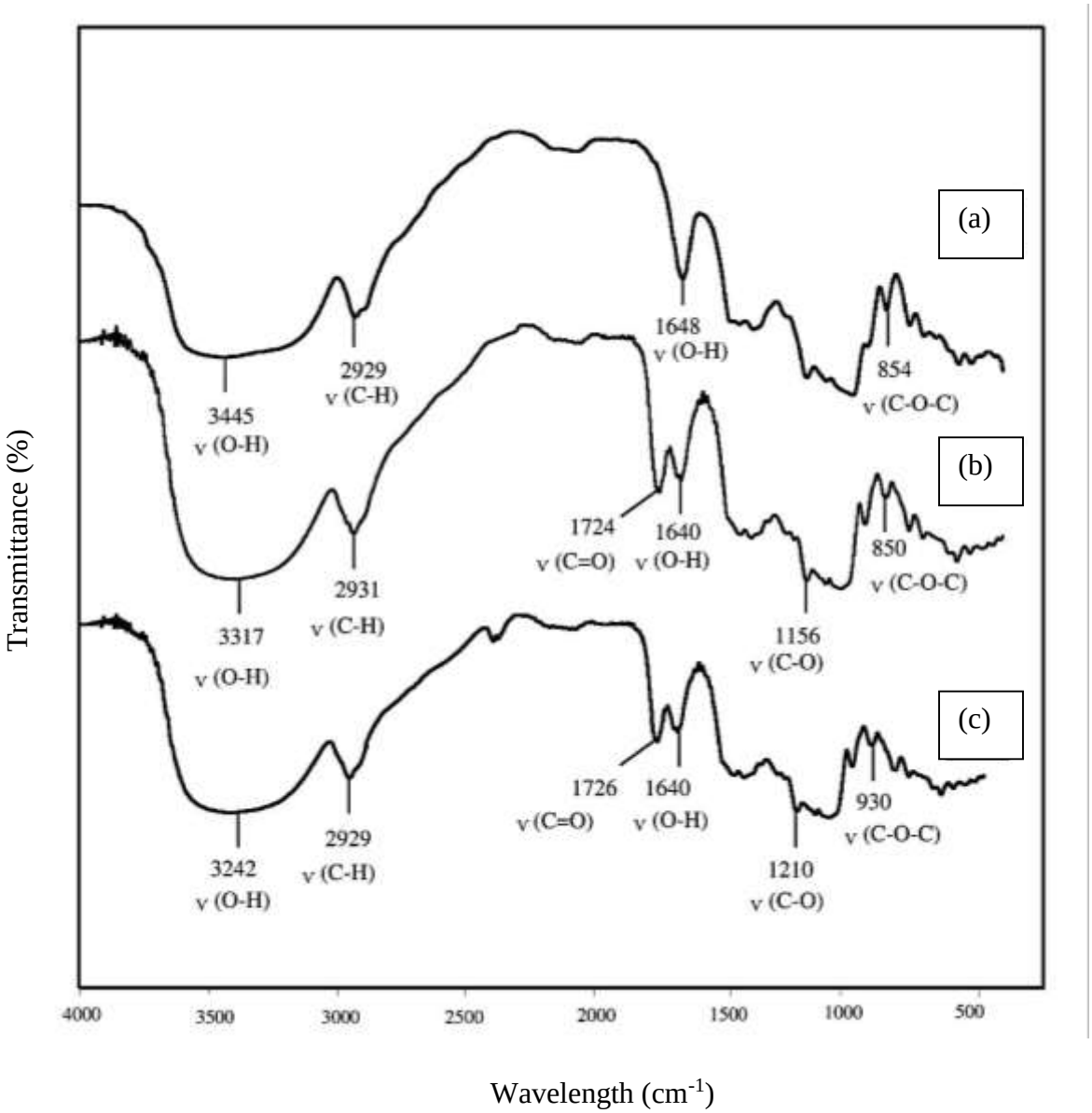

Fig. 2. FTIR spectra of (a) native starch, (b) starch-citrate molecule and (c) starch-citrate nanoparticles

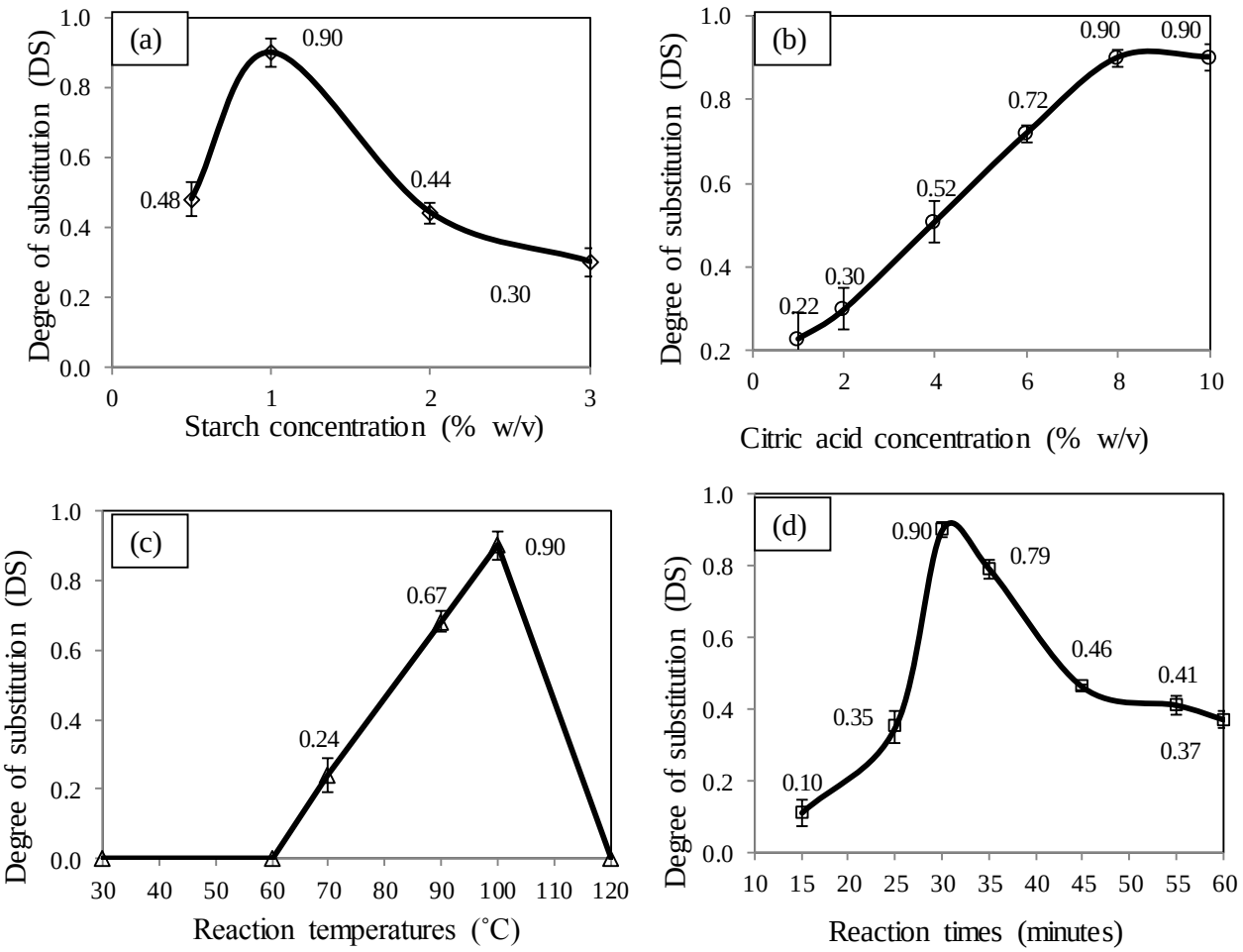

Fig. 3. Effect of synthesis conditions on the degree of substitution (DS) of starch-citrate molecules: (a) starch concentration, (b) citric acid concentration, (c) reaction temperatures and (d) reaction times

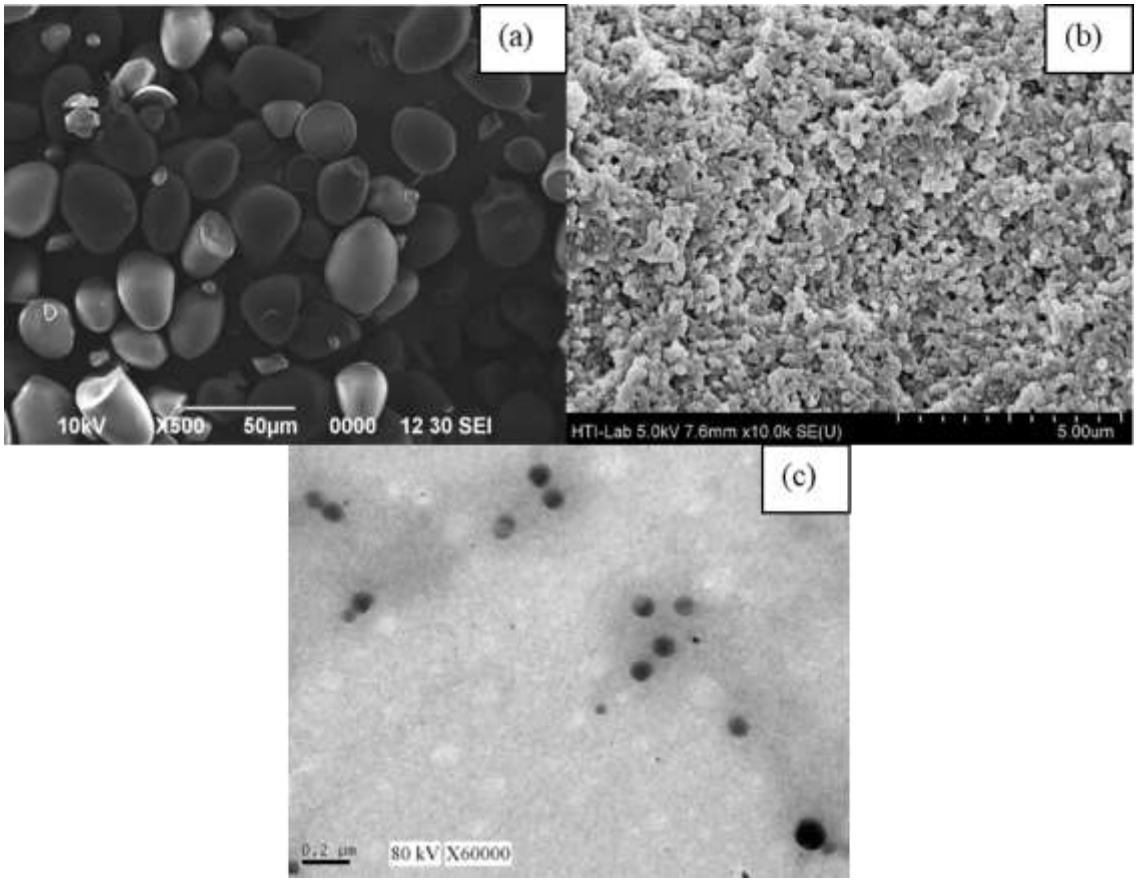

Fig. 4. (a) SEM image of native starch granules; (b) FESEM and (c) TEM images of starch-citrate nanoparticles (DS of 0.9)

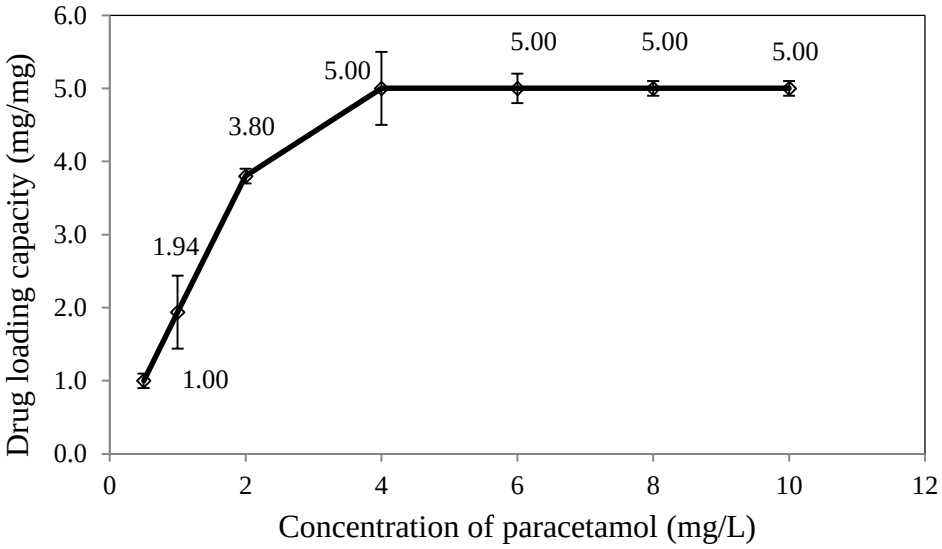

Fig. 5. Paracetamol-loading capacity of starch-citrate nanoparticles

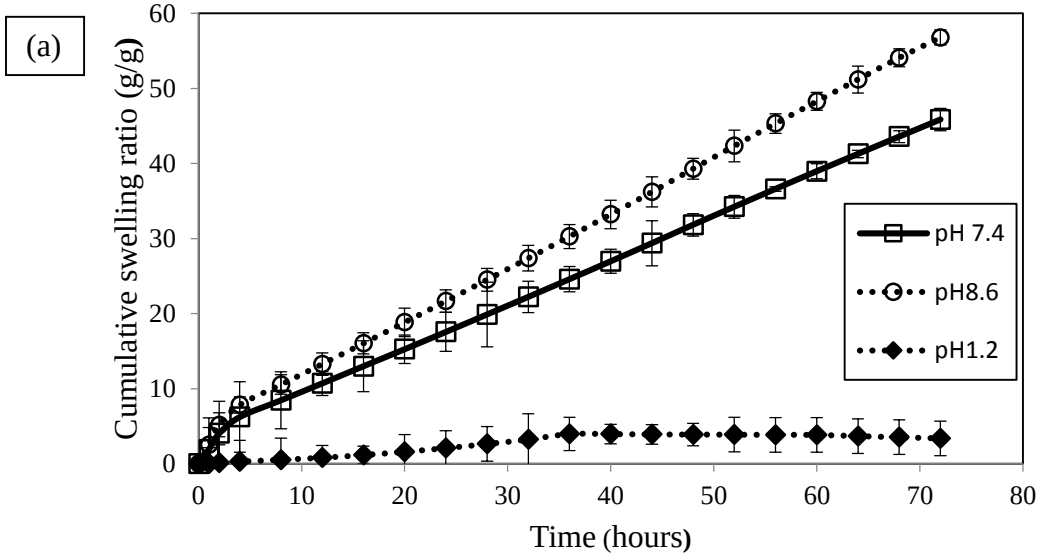

Fig. 6(a). Swelling ratios of starch-citrate nanoparticles in different pH of physiological media (1.2, 7.4 and 8.6) as a function of time

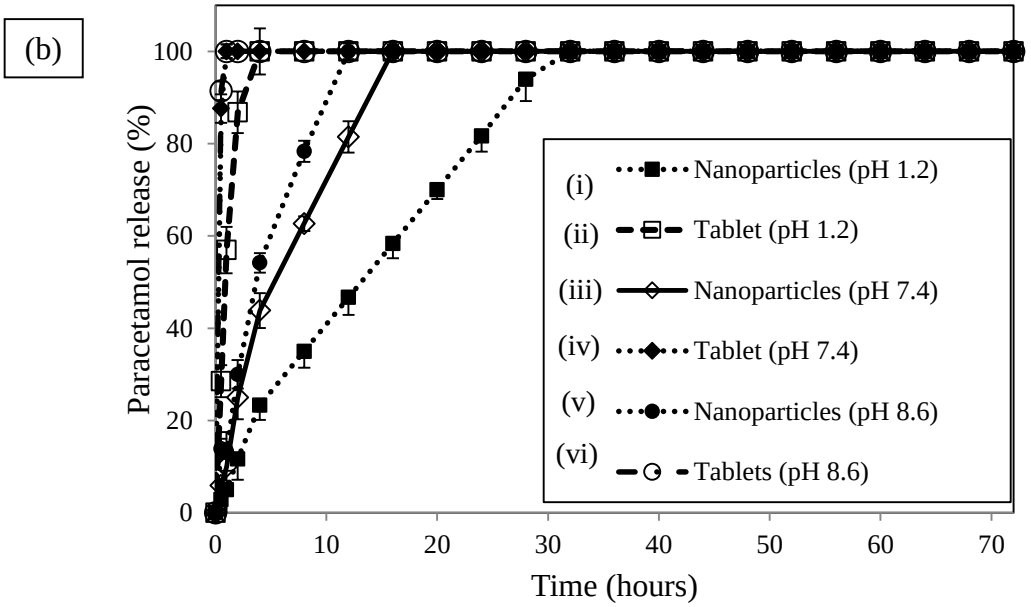

Fig. 6(b). Percentage of paracetamol released from starch-citrate nanoparticles and tablets in media of various pH

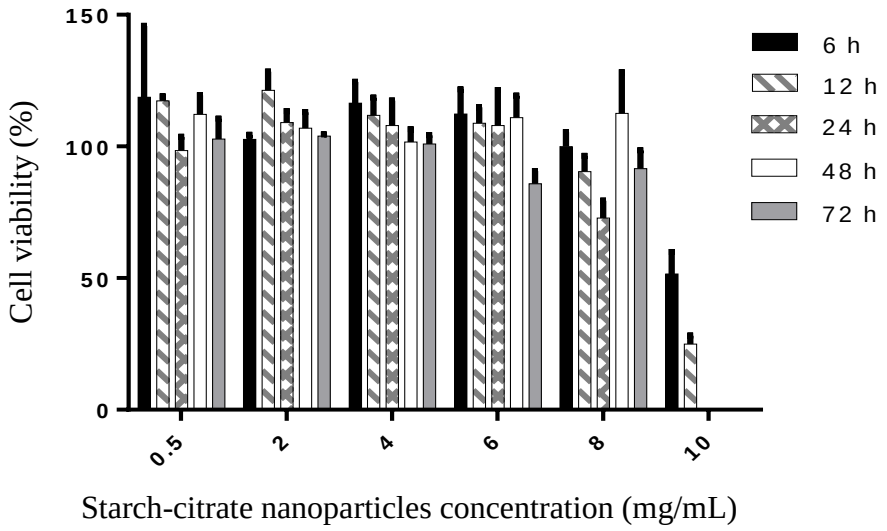

Fig. 7. Cell viability of HaCaT cells cultured with various starch-citrate nanoparticles concentration for 6-72 hours

Table 1: Kinetics modeling of drug release studies of paracetamol-loaded starch-citrate nanoparticles.

pH	Kinetic models	R^2	Features
1.2	Zero order	0.9905	Drug release rate is concentration-independent
7.4		0.9701	
8.6		0.9587	
1.2	First order	0.8222	Drug release rate is concentration-dependent
7.4		0.8359	
8.6		0.8920	
1.2	Hixson-Crowell	0.9043	Drug release mechanism : Surface erosion and swelling
7.4		0.9256	
8.6		0.9263	
1.2	Higuchi	0.9887	Drug release mechanism : Diffusion
7.4		0.9962	
8.6		0.9957	
1.2	Korsmeyer-Peppas	0.9889, n= 0.8434	Drug release mechanism: Diffusion and swelling
7.4		0.9687, n= 0.8800	
8.6		0.9717, n= 0.8533	